Article

The Role of Distance in Singlet Oxygen Applications: A Model System

Matthias Klaper, Werner Fudickar, and Torsten Linker

J. Am. Chem. Soc., **Just Accepted Manuscript** • DOI: 10.1021/jacs.6b01555 • Publication Date (Web): 17 May 2016

The Role of Distance in Singlet Oxygen Applications: A Model System

Matthias Klaper, Werner Fudickar, and Torsten Linker*

Department of Chemistry, University of Potsdam, Karl-Liebknecht-Str. 24-25, 14476 Golm, Germany

Singlet oxygen, intramolecular transfer, distance dependence, quenching and competition experiments

ABSTRACT: Herein, we present a model system which allows the investigation of a directed intramolecular singlet oxygen ($^1O_2$) transfer. Furthermore, we show the influence of singlet oxygen lifetime and diffusion coefficient (D) on the preference of the intra- over the intermolecular reaction in competition experiments. Finally, we demonstrate the distance dependence in quenching experiments, which enables us to draw conclusions about the role of singlet oxygen and $^1O_2$ carriers in PDT.

Introduction

Singlet oxygen ($^1O_2$)[1] is a very convenient oxidant in organic chemistry and can undergo different reactions such as Schenck-Ene reactions,[2] [2+2][3]- and [4+2]-cycloadditions.[4] It can be generated from its ground state by photosensitization using sensitizers like tetraphenylporphyrin (TPP),[5] from inorganic sources (H_2O_2),[6] or with $^1O_2$ donors like naphthalene endoperoxides.[7]

It has also become very important for the treatment of cancer,[8] where it is used in photodynamic therapy (PDT).[9] This technique relies on the precise localization of a sensitizer close to the tumor cells, which are selectively destroyed by light induced formation of reactive oxygen species (ROS) including $^1O_2$. One major drawback of PDT is its lack in selectivity towards the target.[10] Owing to its high reactivity, $^1O_2$ destroys healthy domains when it is either generated or has traveled into these domains.[11] Fortunately, the short lifetime of $^1O_2$ prevents it from travelling larger distances. The lifetime τ is inversely related to rates of deactivation processes arising from physical and chemical interactions with the environment (Scheme 1).

Scheme 1. Modes of Deactivation of $^1O_2$

$$^1O_2 + \text{solvent} \xrightarrow{k_d} {}^3O_2$$

$$^1O_2 + \text{M} \xrightarrow{k_q} {}^3O_2$$

$$^1O_2 + \text{M} \xrightarrow{k_r} MO_2$$

$$k_T = k_q + k_r \qquad \tau = (k_d + k_T[\text{M}])^{-1}$$

The physical quenching by the solvent (k_d) is an unimolecular reaction whereas chemical reactions (k_r) and the physical deactivation (k_q) with substrates M are bimolecular. The lifetime τ limits the range d where $^1O_2$ can exist, which correlates with its diffusion coefficient D ($d=\sqrt{2\tau D}$). Using literature data this gives a value of d=125 nm in water at ambient temperature.[12] The inhomogeneity of a cell is distorting the picture of a uniform diffusion of $^1O_2$ and the efficiency of a transfer of this reactive species depends on the localization of the sensitizer, being either close (direct transfer) or remote (indirect transfer) from the target (Figure 1).

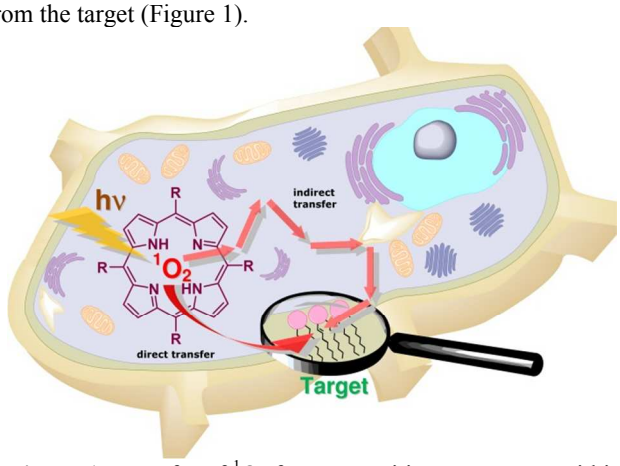

Figure 1. Transfer of $^1O_2$ from a sensitizer to a target within a cell.

In cells, chemical reactions of $^1O_2$ with amino acids of proteins, unsaturated lipids, or nucleic acids are effectively reducing its lifetime.[13] In addition, diffusion coefficients are varying strongly inside the cell. Several strategies where performed in order to determine the effective range d in cells: The group of Ogilby tackles the question by spatially resolving $^1O_2$ in cells based on the microscopic imaging of the $^1O_2$ phosphorescence.[14] Surprisingly, the lifetimes measured inside the cell were long, suggesting that chemical quenching processes are negligible. On the other hand, different subcellular domains restrict traveling of $^1O_2$, possibly due to different viscosities

inside the cell.[14b] Other strategies were followed by Moan and Berg, who studied intracellular photo-degradation processes of two dyes which could be excited selectively at different wavelengths.[15] Their results revealed that singlet oxygen causes damage rather at the dye where it is generated than at the dye which is not sensitizing. They estimated a travel distance of only 10-20 nm.

A third strategy comprises the investigation of model systems where $^1O_2$ is transferred within one molecule or within a molecular assembly (intramolecular reaction). Such systems would constitute both, the photosensitizer and the $^1O_2$ target in one entity and would principally resemble modern PDT delivery vehicles, which convey the sensitizer close to the tumor tissue.[9a]

A single molecule atomic force microscopy study of a system was performed, where a sensitizer and $^1O_2$ cleavable linkers were located on a 2D DNA origami.[16] The sensitizer generated $^1O_2$ which caused chain scission at different positions. For the first time, it was possible to monitor the behavior of $^1O_2$ in the nanometer range. It was shown that the closer linker was stronger affected than the further remote one under irradiation of the sensitizer.

Shu, To and Fadul developed an imaging technology, where large protein complexes were inserted between a singlet oxygen sensor and generator.[17] Their method allowed confirming the topology of protein complexes owing to a distance dependent $^1O_2$ transfer.

Very recently, our group investigated such a transfer by using a chemical donor of $^1O_2$ connected to an acceptor unit.[18] In this study, only one molecule $^1O_2$ could be donated from the carrier to the acceptor. In competition experiments with a second non-bound acceptor molecule it was found that the intramolecular transfer prevails depending on the molecular conformation, the temperature and the solvent depended lifetime of $^1O_2$. However, the scope of these experiments was limited by the fact that a maximum of only one equivalent of $^1O_2$ is available from the donor.

Herein we demonstrate how an intramolecular reaction is controlled in a sensitizer-acceptor system (**SAS**), where the reactive species can be generated continuously. We will address both, the questions of dependence on the distance and on the surrounding environment which will reveal important insights to PDT (Figure 1).

Results and discussion

We decided to employ a sensitizer-acceptor system (**SAS**), which carries a porphyrin functioning as the $^1O_2$-sensitizing unit and an alkene functioning as the $^1O_2$ acceptor. Both units are connected by alkyl spacers at various chain lengths (**SAS0–6**) for n=0–6 separating the site where $^1O_2$ is generated from the site where it is trapped at varying distances.

For the sensitizing part, we used a hydroxy-substituted tetraphenylporphyrin (TPP), since it has a high $^1O_2$ quantum yield and is easily accessible.[19] The acceptor is a trimethyl-substituted alkene bound to the termini of spacer units with varying chain lengths (n=0–6). Therefore, porphyrin **1**[20] and the bromo compounds **2**[21] were synthesized according to literature procedures and linked together *via* a Williamson ether synthesis (Scheme 2, Supporting Information). The alkene undergoes a Schenck-Ene reaction with $^1O_2$ to give hydroperoxides **SASO2a** and **SASO2b** as a mixture of two regioisomers.[22] Compared to the donor/acceptor systems, used in our previous work,[18] these photooxygenations can run to full conversion since $^1O_2$ is generated continuously. In addition to the synthesis of **SAS**, it is necessary to have a reference system (**RS**) which carries only the acceptor unit and the spacer with a phenyl terminus without the sensitizing unit. To avoid different $^1O_2$ quantum yields, we carried out all photooxygenations of **RS** with a 1:1 mixture of the corresponding **RS/SAS**, where $^1O_2$ is always generated by the porphyrin unit of **SAS** linked to an alkyl chain.[23] The **RS** would resemble the typical situation of an intermolecular reaction while **SAS** combines both, inter- and intramolecular reactions. Our aim in this study is to control and estimate the contributions of these two reactions in **SAS**.

Scheme 2. Syntheses of SAS- and Reference Systems (RS) and Subsequent Schenck-Ene Reactions to Hydroperoxides

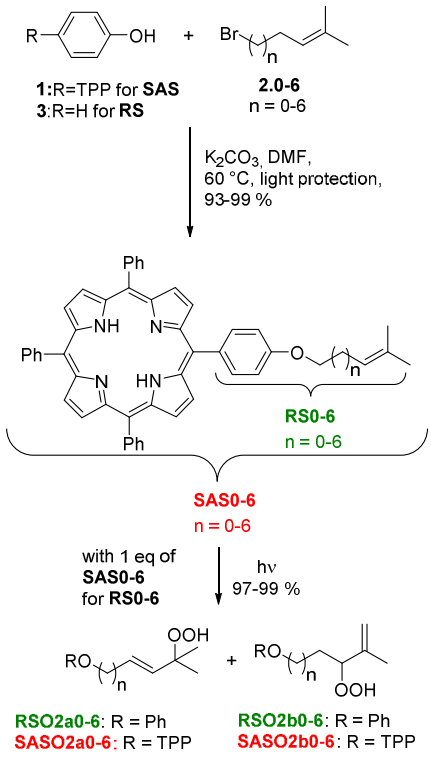

At first, we paid our attention to **RS**. During irradiation in the presence of ambient atmospheric oxygen of $5 \cdot 10^{-5}$ M solutions of both, **RS** and the corresponding sensitizer,[23] in acetonitrile (MeCN) the consumption of starting material was followed by HPLC. The semi-logarithmic plot of the concentration versus time gives a straight line which is in accordance with a pseudo first order reaction (Figures SI). The slope equals the observed rate constant k_{obs} which can be expressed by the following equation.[24]

$$\ln[A]_t = \ln[A]_0 - (v_F k_r / k_d) \cdot t = \ln[A]_0 - k_{obs} \cdot t \quad (1)$$

Here, [A] is the concentration of the substrate (**RS**) and v_F is the production of $^1O_2$ (its determination is described in detail

in the SI, giving a value of $3.6 \cdot 10^{-5}$ Ms^{-1} for all following experiments). Note that any other quenching process as mentioned in Scheme 1 is neglected since $k_d >> k_T[A]$. The bimolecular constants k_r of the seven **RS0–6** in MeCN ($k_d = 1.5 \cdot 10^4$ s^{-1})[25] were calculated from equation 1 and are summarized in Table 1. With exception of the more slowly reacting sterically hindered **RS0**, the values alternate between $1\text{-}1.7 \cdot 10^5$ $M^{-1}s^{-1}$. Compounds **RS1**, **3** and **5** with an even number of methylene groups between the oxygen atom and the olefinic unit are reacting faster than compounds **RS2**, **4** and **6** with an odd number. Odd-even effects are known to affect molecular properties such as packing, solubility and phase transitions as well.[26]

Table 1. Bimolecular Rate Constants k_r of the Schenck-Ene Reactions of RS in Acetonitrile and Ethanol

entry	RS	n	k_r (MeCN)/ 10^4 $M^{-1}s^{-1}$	k_r (EtOH)/ 10^4 $M^{-1}s^{-1}$
1	RS0	0	1.5±0.1	1.5±0.1
2	RS1	1	15.3±0.1	13.9±0.2
3	RS2	2	9.97±0.1	10.4±0.3
4	RS3	3	17.3±0.2	16.1±0.2
5	RS4	4	9.64±0.1	8.3±0.2
6	RS5	5	16.1±0.1	11.3±0.3
7	RS6	6	10.1±0.1	7.4±0.2

Next, photooxygenations were carried out under the same conditions with **SAS**. The slopes of the semi-logarithmic plots of **SAS0–6** are indeed steeper as for the corresponding **RS0–6** (Figure 2a, S2–8, Table 2). For SAS the odd-even effects are preserved at the same degree as for **RS**. It is important to note that the comparison between **RS** and **SAS** assumes essentially identical values for k_r, since the reactive centers are identical. To support this postulate, the geometries of **SAS0–6** were optimized by DFT calculations (see SI). In such calculations all **SAS** are linearly stretched, depicting the reacting olefinic moiety isolated from the pendant macrocycle. Although in solution the alkyl chain should be more flexible, the above described odd-even effect speaks for a stretched and not bended chain. We can therefore conclude that electronic and steric influences on these centers are nearly identical. Thus, the observed rate constants k_{obs} for a photooxygenation with a partial contribution of an intramolecular $^1O_2$ transfer are slightly increased for **SAS**. This change is the result of the smaller degree of solvent quenching since k_d reduces the overall rate k_{obs}.

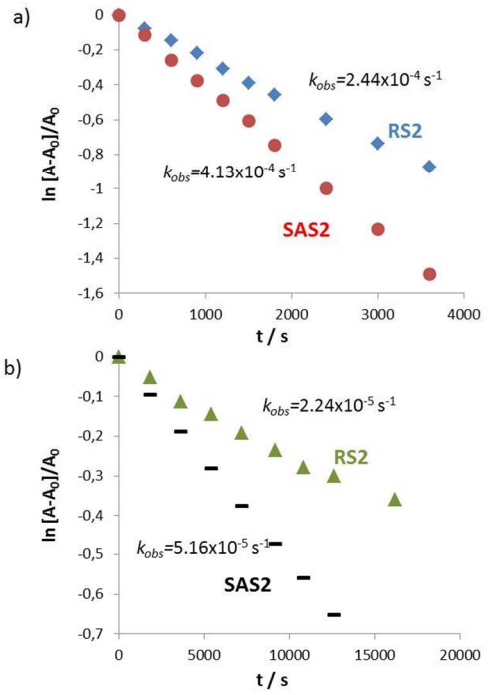

Figure 2. Observed rates of the photooxygenation depicted as semi logarithmic plots: a) **RS2** (blue) and **SAS2** (red) in MeCN; b) **RS2** (green) and **SAS2** (black) in EtOH.

Table 2. Observed Rate Constants k_{obs} of RS and SAS in Acetonitrile and Ethanol

n	**RS** MeCN k_{obs}/ $10^{-5}s^{-1}$	**SAS** MeCN k_{obs}/ $10^{-5}s^{-1}$	k_{SAS}/ k_{RS}	**RS** EtOH k_{obs}/ $10^{-5}s^{-1}$	**SAS** EtOH k_{obs}/ $10^{-5}s^{-1}$	k_{SAS} /k_{RS}
0	3.74±0.1	5.11±0.1	1.36	0.37±0.01	0.74±0.01	1.98
1	37.3±0.1	49.8±0.1	1.33	2.48±0.01	6.96±0.03	2.80
2	24.4±0.1	41.3±0.1	1.69	2.24±0.01	5.16±0.01	2.31
3	42.3±0.5	57.8±0.8	1.35	4.17±0.07	7.75±0.06	1.83
4	23.6±0.7	31.1±0.5	1.30	2.78±0.47	4.18±0.02	1.50
5	39.3±0.4	49.9±0.2	1.27	3.77±0.02	5.68±0.03	1.50
6	25.4±0.3	36.8±0.3	1.22	2.48±0.04	3.69±0.02	1.48

Consequently, the impact of an intramolecular reaction should become more pronounced when solvent quenching is stronger and k_d is increased. We therefore switched the solvent system to ethanol ($k_d = 7.2 \cdot 10^4$ s^{-1}).[25] As expected, the observed rates are strongly reduced as compared to the solvent MeCN but the differences in the slopes between **RS** and **SAS** are increased (Figure 2b, Table 2). Quantitatively, the effect of an intramolecular reaction can be expressed by the ratio of the observed rate constants k_{SAS}/k_{RS}. From Table 2 it becomes clear that this effect is becoming stronger with increasing solvent quenching.

The biasing of an intramolecular reaction reaches a limit with water as the most quenching solvent ($k_d = 3.2 \cdot 10^5$ s^{-1}).[25] However, the solvent water is incompatible with our systems. The domination of the intramolecular reaction of **SAS** should become further increased, when the intermolecular reaction of

SAS has to compete with another intermolecular reaction arising from a second substrate which reacts with $^1O_2$ at a higher rate. Thus, we chose tetramethylethylene (TME), an extremely reactive substrate towards $^1O_2$ (k_r=5.6·10^7 M^{-1}s^{-1}).[24] Accordingly, the lifetime of $^1O_2$ is reduced to 1.7 µs which is less than its lifetime in water (3-5 µs).[24] Photooxygenation of TME leads to one single hydroperoxide which does not undergo further transformations under the present conditions.[27] Thus, although organic hydroperoxides are associated with oxidative damages in biologic systems,[28] they suit well for our model systems.

As described before, irradiation was now carried out in the presence of TME at a concentration of 10^{-2} M. The results of these competition experiments are summarized in Table 3. Here, the intermolecular reaction is suppressed by magnitudes as reflected by the high values of k_{SAS}/k_{RS}.

The alternation pattern of reactivities found in the two former cases with no TME is reduced but still present. More importantly, the ratio of intra- *versus* intermolecular reactions (k_{SAS}/k_{RS}) decreases remarkably with increasing *n* (Figure 3, Table 3). Thus, we can give evidence for a relationship between the prevalence of intramolecular reaction and the distance. By means of the calculated structures (see SI), the distances between sensitizer and acceptor increase from 12 Å to 19.5 Å from **SAS1** to **SAS6**. According to Figure 3 the dominance of intramolecular transfer would drop to k_{SAS}/k_{RS}=1 at 7-8 methylene groups (≥2 nm). The travel distance of a $^1O_2$ molecule before quenching under the given conditions is $d=\sqrt{(2k^{-1}D)}$, where *k* includes all quenching processes and D=9.2·10^{-9} m^{2}s^{-1}. This gives a value of d=176 nm. Therefore, the travel distance of $^1O_2$ is still by magnitudes higher than the molecular dimensions of **SAS**.

Table 3. Observed Rate Constants k_{obs} of RS and SAS in the Presence of TME (200eq) in Acetonitrile

entry	n	RS k_{obs}/ $10^{-5}s^{-1}$[a]	SAS k_{obs}/ $10^{-5}s^{-1}$	factor k_{SAS}/k_{RS}
1	0	0.04	4.92±0.01	119
2	1	0.24	28.51±0.01	118
3	2	0.24	27.53±0.02	113
4	3	0.26	26.86±0.4	103
5	4	0.15	13.81±0.02	91
6	5	0.23	16.51±0.01	70
7	6	0.12	4.64±0.05	38

[a]Error=±0.01

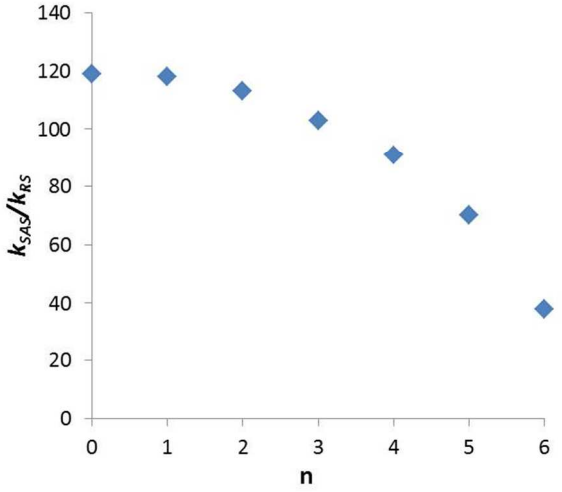

Figure 3. Preference of intra- over intermolecular reaction (k_{SAS}/k_{RS}) in the presence of TME as a function of *n*.

In addition to the revelation of the chain length dependence, we focused on a quantification of the influence of quenchers on biasing an intramolecular reaction in a system such as **SAS** as well. Therefore, we first evoke equation (2), which expresses an intermolecular oxygenation of a substrate A in the presence of a second competing substrate A' in excess. This formula should be suitable to calculate the rate constants of the photooxygenations by knowledge of k_r, k_d and k'_r.[24]

$$\ln[A]_t=\ln[A]_0-(v_F k_r/(k_d+k'_r[A']))\cdot t=\ln[A]_0-k_{obs}\cdot t \quad (2)$$

Considering the concentration of [*A*'] as constant (0.01 M) and using 1.5·10^4 s^{-1} for k_d, 5.6·10^7 M^{-1}s^{-1} for k'_r (TME) and the k_r values for **RS** from Table 1, we obtain k_{obs} ranging between 6.3·10^{-6} and 10.7·10^{-6} s^{-1}. Thus, the expected theoretical values for k_{obs} are higher than the measured values ranging only between 1.2·10^{-6} and 2.6·10^{-6} s^{-1} (see Table 3). This can be a result from underestimated chemical quenching of TME at this high concentration and from the products generated from the oxygenation of TME. In contrast, if assuming a genuine intramolecular reaction which is essentially free from any competing reactions and from solvent quenching, the simple equation (3) should become valid.

$$\ln[A]_t=\ln[A]_0-v_F k_r\cdot t=\ln[A]_0-k_{obs}\cdot t \quad (3)$$

The expected theoretical values for k_{obs} would therefore range between 3.6 and 6.1 s^{-1} as compared to the observed rates of **SAS** of 0.4 to 2.8·10^{-4} s^{-1}. This strong deviation (factor ≈10^4) shows that quenching processes still occur for the intramolecular reaction under our experimental conditions. Note that k_{obs} calculated from equation (3) deviates of course much stronger for **RS** (factor ≈10^6). Even at the shortest distance, **SAS1** reacts far too slow. This may be explained by picturing the environment around a new born $^1O_2$ molecule from a **SAS**. We can consider a hypothetical sphere with the radius *d* (176 nm as calculated above), centered at the point where $^1O_2$ was generated. From this point $^1O_2$ can travel into any direction and can either hit the reactive site or abandon the sphere to be

deactivated. However, the reactive site covers only a small sector within the sphere and all other deviating travel directions would cause the loss of $^1O_2$ (Figure 4). Therefore, geometry depending factors become effective, which are also used for example, for expressing the Förster critical distance.[29] It becomes clear, that a quantitative intramolecular process would be realized only when the sensitizer is connected with multiple acceptors in a 3D dendrimeric structure, covering the entire inner part of the sphere. Thus, the reactions of **SAS** proceed slower as expressed in equation (3). This model explains also why the intramolecular prevalence fades out at considerably smaller chain lengths: We may therefore consider spheres with radii r corresponding to the diameters of **SAS**. **SAS0**, for example, would give V≈7nm^3, and **SAS6** would give V≈32nm^3. Importantly, the volume covered by the reactive centers is the same. Thus, the ratio between the space covered by the reactive space and the total volume drops with r^3.

From these observations we can draw the following conclusions: An oxygenation reaction where one molecule $^1O_2$ is attacking exclusively at a site where its generated (either from the same molecule or intermoleculary but within the vicinity of the sensitizer) can be realized only by the use of strong competing quenchers, requiring $k_{quencher}[A_{quencher}] >> k_r$ and a distance between sensitizer and reactive site $<< \sqrt{(2k_{quencher}{}^{-1}D)}$ (see Scheme 1). Fulfillment of these requirements would indeed reduce intermolecular reactions below 1%. On the other hand, the time required for a complete oxidation is increased which can be predicted using equation (3). For PDT applications benign quenchers might be available, which protect healthy regions from damage by $^1O_2$. As the main challenge remains the accomplishment of the required proximity between sensitizer and target for a true intramolecular process. The distance dependence found in this work reveals that this proximity is by magnitudes smaller than expected.

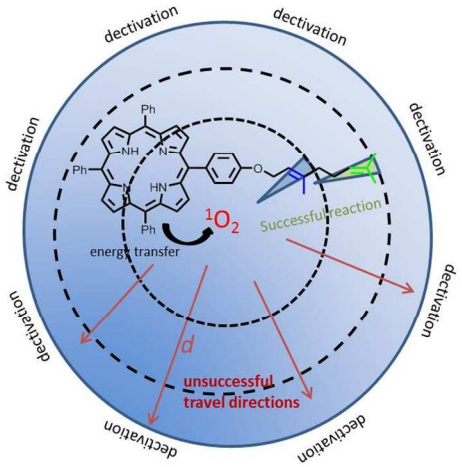

Figure 4. Relationship between the diffusion range d of $^1O_2$, solvent collisions, and the possibility of an intramolecular reaction. The inner circle depicts the dimensions of a smaller spherical space where collisions occur at closer intramolecular distances (highlighted blue), the circle in the middle depicts a larger sphere for larger distances (highlighted green), outermost circle depicts the maximum travel distance of $^1O_2$ before its deactivation.

Conclusion

In summary, we synthesized several sensitizer-acceptor systems with different *intra*molecular distances. The observed rates of their photooxygenations in acetonitrile under continuous irradiation are moderately higher than rates of analogous intermolecular reactions. By using ethanol as solvent, with higher $^1O_2$ quenching rate, the ratio of intra- *versus* intermolecular oxidation increases. The most dramatic increase of this ratio by a factor of ≈120, however, is achieved by using an additional chemical $^1O_2$ quencher. We have presented a quantitative relation of k_{intra}/k_{inter} to chemical rate constants, concentrations and solvent parameters.

In addition, we have shown a strong impact of the distance on this preference in the highly quenching solvent system. For the design of such a sensitizer-acceptor molecule, the distance should not exceed 2 nm. These experimental findings are not conflicting with the much higher predictable travel distance of $^1O_2$ derived from its lifetime and diffusion coefficient: A $^1O_2$ molecule generated in the proximity of a reactive site is not inevitably causing a reaction but can travel in other directions. Thus, the sole intramolecular process would require a special 3D molecular architecture, where any travel direction of $^1O_2$ would lead to a successful encounter. This insight helps to understand the relations between diffusion, lifetime and chemical efficiency of $^1O_2$ in PDT.

ASSOCIATED CONTENT

Supporting Information. Experimental procedures and characterization data, sample preparation, determination of k-values including plots of c/c_0 *versus* t, NMR spectra, and quantum chemical calculations. This material is available free of charge via the Internet at http://pubs.acs.org.

AUTHOR INFORMATION

Corresponding Author

*linker@uni-potsdam.de

ACKNOWLEDGMENT

We thank the University of Potsdam for generous financial support. We thank Dr. Heidenreich for assistance in NMR analysis and Dr. Starke for measurement of mass spectra.

REFERENCES

(1) (a) *Singlet Oxygen*; Frimer, A. A.; Ed.; CRC Press: Boca Raton, 1985. (b) *Handbook of Synthetic Photochemistry: Singlet Oxygen as a Reagent in Organic Synthesis;* Greer, A.; Zamadar, M., Ed.; Wiley-VCH: Weinheim, 2010. (c) Ogilby, P. R. *Chem. Soc. Rev.* **2010**, 39, 3181–3209.
(2) Adam, W.; Bosio, S. G.; Turro, N. J.; Wolff, B. T. *J. Org. Chem.* **2004**, *69*, 1704–1715.
(3) Adam, W.; Bosio, S. G.; Turro, N. J. *J. Am. Chem. Soc.* **2002**, *124*, 8814–8815.
(4) Adam, W.; Prein, M. *Acc. Chem. Res.* **1996**, *29*, 275–283.
(5) (a) Cló, E.; Snyder, J. W.; Voigt, N. V.; Ogilby, P. R.; Gothelf, K. V. *J. Am. Chem. Soc.* **2006**, *128*, 4200–4201. (b) Frederiksen, P. K.; McIlroy, S. P.; Nielsen, C. B.; Nikolajsen, L.; Skovsen, E.; Jørgensen, M.; Mikkelsen, K. V.; Ogilby, P. R. *J. Am. Chem. Soc.* **2005**, *127*, 255–269. (c) Tørring, T.; Toftegaard, R.; Arnbjerg, J.; Ogilby, P. R.;

Gothelf, K. V. *Angew. Chem., Int. Ed.* **2010**, *49*, 7923–7925. (d) McQuade, D. T.; Seeberger, P. H. *J. Org. Chem.* **2013**, *78*, 6384–6389.
(6) (a) Aubry, J.-M.; Bouttemy, S. *J. Am. Chem. Soc.* **1997**, *119*, 5286–5294. (b) Wahlen, J.; de Vos, D. E.; Groothaert, M. H.; Nardello, V.; Aubry, J.-M.; Alsters, P. L.; Jacobs, P. A. *J. Am. Chem. Soc.* **2005**, *127*, 17166–17167. (c) Pierlot, C.; Nardello, V.; Schrive, J.; Mabille, C.; Barbillat, J.; Sombret, B.; Aubry, J.-M. *J. Org. Chem.* **2002**, *67*, 2418–2423.
(7) (a) Klaper, M.; Linker, T. *Chem. Eur. J.* **2015**, *21*, 8569–8577. (b) Martinez, G. R.; Ravanat, J.-L.; Medeiros, M. H. G.; Cadet, J.; Di Mascio, P. *J. Am. Chem. Soc.* **2000**, *122*, 10212–10213. (c) Pierlot, C.; Hajjam, S.; Barthélémy, C.; Aubry, J.-M. *J. Photochem. Photobiol. B: Biol*. **1996**, *36*, 31–39.
(8) (a) Cló, E.; Snyder, J. W.; Ogilby, P. R.; Gothelf, K. V. *ChemBioChem* **2007**, *8*, 475–481. (b) Kuimova, M. K.; Yahioglu, G.; Ogilby, P. R. *J. Am. Chem. Soc.* **2009**, *131*, 332–340. (c) Dougherty, T. J.; Gomer, C. J.; Henderson, B. W.; Jori, G.; Kessel, D.; Korbelik, M.; Moan, J.; Peng, Q. *J. Natl. Cancer Inst.* **1998**, *90*, 889–905. (d) Henderson, B. W.; Dougherty, T. J. *Photochem Photobiol*. **1992**, *55*, 145–157.
(9) (a) Moor, A. C. E.; Ortel, B.; Hasan, T.; *Photodynamic Therapy;* Patrice, M. Ed.; Royal Society of Chemistry: Cambridge, 2003; Ch. 2, pp19–58. (b) Bonnett, R. *Chem. Soc. Rev.* **1995**, *24*, 19–33. (c) Bartusik, D.; Aebisher, D.; Ghogare, A.; Ghosh, G.; Abramova, I.; Hasan, T.; Greer, A. *Photochem. Photobiol.* **2013**, *89*, 936–941. (d) Tromberg, B.; Kimel, S.; Orenstein, A.; Barker, S.; Hyatt, J.; Nelson, J.; Roberts, W.; Berns, M. *J. Photochem. Photobiol. B: Biol*. **1990**, *5*, 121–126.
(10) Orensten, A.; Kostenrich, G.; Roitman, L.; Shechtman, Y.; Kopolovic, Y.; Ehrenberg, B.; Maic, Z. *Br. J. Cancer* **1996**, *73*, 937–944.
(11) Davis, M. J. *Photochem. Photobiol. Sci.* **2004**, *3*, 17–25. (b) Doleiden, F. H.; Fahrenholtz, S. R.; Lamola, A. A.; Trozzolo, A. M. *Photochem. Photobiol.* **1974**, *20*, 519–521. (c) Sies, H.; Menck, C. F. M. *Mutat. Res*. **1992**, *275*, 367–315.
(12) (a) Hatz, S.; Poulsen, L.; Ogilby, P. R. *Photochem. Potobiol.* **2008**, *84*, 1284–1290. (b) Skovsen, E.; Snyder, J. W.; Lambert, J. D. C.; Ogilby, P. R. *J. Phys. Chem. B* **2005**, *109*, 8570–8573.
(13) Redmond, R. W.; Kochevar, I. E. *Photochem. Photobiol.* **2006**, *82*, 1178–1186.
(14) (a) Breitenbach, T.; Kuimova, M. K.; Gbur, P.; Hatz, S.; Schack, N. B.; Pedersen, B. W.; Lambert, J. D. C.; Poulsen, L.; Ogilby, P. R. *Photochem. Photobiol. Sci.*, **2009**, *8*, 442–452. (b) Snyder, J. W.; Skovsen, E.; Lambert, J. D. C.; Poulsen, L.; Ogilby, P. R. *Phys. Chem. Chem. Phys.* **2006**, *8*, 4280–4293. (c) Ogilby, P. R. *Photochem. Photobiol. Sci.* **2010**, *9*, 1543–1560. (d) Kuimova, M. K.; Yahioglu, G.; Ogilby, P. R. *J. Am. Chem. Soc.* **2009**, *131*, 332–340.
(15) Moan, J.; Berg, K. *Photochem. Photobiol.* **1991**, *53*, 549**–**553.
(16) a) Voigt, N. V.; Tørring, T.; Rotaru, A.; Jacobsen, M. F.; Ravnsbaek, J. B.; Subramani, R.; Mamdouh, W.; Kjems, J.; Mokhir, A.; Besenbacher, F.; Gothelf, K. V. *Nat. Nanotechnol.* **2010**, *5*, 200–203. (b) Helmig, S.; Rotaru, A.; Arian, D.; Kovbasyuk, L.; Arnbjerg, J.; Ogilby, P. R.; Kiems, J.; Mokhir, A.; Besenbacher, F.; Gothelf, K. V. *ACS Nano* **2010**, *4*, 7475–7480. (c) Tørring, T.; Helmig, S.; Ogilby, P. R.; Gothelf, K. V. *Acc. Chem. Res.* **2014**, *47*, 1799–1806.
(17) To, T.-L.; Fadul, M. J.; Shu, X. *Nature Commun.* **2014**, *5*, 4072**–**4080.
(18) Klaper, M.; Linker, T. *J. Am. Chem. Soc.* **2015**, *137*, 13744–13747.
(19) Bonnett, R.; McGarvey, D. J.; Harriman, A.; Land, E. J.; Truscott, T. G.; Winfield, U.-J. *Photchem. Photobiol.* **1988**, *48*, 271–276.
(20) Borocci, S.; Marotti, F.; Mancini, G.; Monti, D.; Pastorini, A. *Langmuir* **2001**, *17*, 7198–7203.
(21) (a) Shresta-Dawadi, P. B.; Lugtenburg, J. *Eur. J. Org. Chem.* **2003**, 4654–4663. (b) Mori, K.; Sugai, T.; Maeda, Y.; Okazaki, T.; Noguchi, T.; Naito, H. *Tetrahedron* **1985**, *41*, 5307–5311. (c) Biernacki, W.; Gdula, A. *Synthesis* **1979**, 37–38.
(22) (a) Adam, W.; Richter, M. J. *J. Org. Chem.* **1994**, *59*, 3335–3340. (b) Brünker, H.-G.; Adam, W. *J. Am. Chem. Soc.* **1995**, *117*, 3976–3982. (c) Adam, W.; Brünker, H.-G.; Kumar, A. S.; Peters, E.-M.; Peters, K.; Schneider, U.; von Schnering, H. G. *J. Am. Chem. Soc.* **1996**, *118*, 1899–1905.
(23) To ensure consistent $^1O_2$ quantum yields for all following kinetic experiments, we used the corresponding SAS with the same chain length as sensitizer.
(24) Wilkinson, F.; Helmann, W. P.; Ross, A. B. *J. Phys. Chem. Ref. Data* **1995**, *24*, 663–1021.
(25) (a) Ogilby, P. R.; Foote, C. S. *J. Am. Chem. Soc.* **1983**, *105*, 3423–3430. (b) Aubry, J.-M.; Mandard-Cazin, B.; Rougee, M.; Bensasson, R. V. *J. Am. Chem. Soc.* **1995**, *117*, 9159–9164.
(26) Tao, F.; Bernasek, S. L. .*Chem. Rev.* **2007**, *107*, 1408–1453.
(27) Dang, H.-S.; Davies, A. G.; Davison, I. G. E.; Schiesser, C. H. *J. Org. Chem.* **1990**, *55*, 1432–1438.
(28) Girotti, A. W. *Lipid Res.* **1998**, *39*, 1529–1542.
(29) Börjesson, K.; Preus, S.; El-Sagheer, A. H.; Brown, T.; Albinsson, B.; Wilhelmsson, L. M. *J. Am. Chem. Soc.* **2009**, *131*, 4288–4293.

Insert Table of Contents artwork here